PCCP

Accepted Manuscript

ROYAL SOCIETY OF CHEMISTRY

www.rsc.org/pccp

σ-hole interaction with radical species as electron donors: Does single-electron tetrel bonding exist?

Qingzhong Li[*,1], Xin Guo[1], Xin Yang[1], Wenzuo Li[1], Jianbo Cheng[1], Hai-Bei Li[*,2]

[1] *The Laboratory of Theoretical and Computational Chemistry, School of Chemistry and Chemical Engineering, Yantai University, Yantai 264005, People's Republic of China*

[2] *School of Ocean, Shandong University, Weihai 264209, People's Republic of China*

***To whom all correspondence should be addressed**:

Dr. Qingzhong Li, E-mail: lqz@ytu.edu.cn

Dr. Hai-Bei Li, E-mail: lihaibei@sdu.edu.cn

Abstract

A single-electron tetrel bond was predicted and characterized in the complexes $FXH_3\cdots CH_3$ (X = C, Si, Ge, and Sn) by performing quantum chemical calculations, where the methyl radical acts as the Lewis base and the σ-hole on the X atom in FXH_3 as the Lewis acid. The interaction between the methyl radical and FXH_3 is characterized with a red shift of F–X stretching frequency. The strength of the tetrel bond becomes stronger with not only increasing the atomic number of central atom X (X = C, Si, Ge, and Sn) but also enhancing the electron-withdrawing ability of substituents in the Lewis acid. The energy decomposition analysis highlights the importance of electrostatic interaction in the formation of the tetrel bond, although the dispersion part is also nonnegligible for the weak tetrel bond. There is a competition between the formation of single-electron tetrel bonds and hydrogen bonds for the complexes composed of the methyl radical and $CNCH_3$ or $NCCH_3$. Furthermore, the single-electron tetrel bond exhibits the cooperative effect not only with the hydrogen bond in the complex of $NCH\cdots NCCH_3\cdots CH_3$, but also with the conventional tetrel bond in $NCCH_3\cdots NCCH_3\cdots CH_3$.

Keywords: Single-electron tetrel bond; Substituents; Cooperativity; Competition; Dispersion energy

1. Introduction

Radicals have been considered to be extremely important as intermediates in many chemical reactions,[1] a typical representative of which is methyl radical. It is frequently detected in combustion chemistry, and also observed in the upper atmosphere of celestial body.[2] Thus, the structure and properties of methyl radical have attracted much attention both theoretically and experimentally.[3-5] The methyl radical exhibits a planar structure with D_{3h} symmetry.[5] The carbon atom in the methyl radical is sp^2-hybridized with one single electron held in a *p* orbital. The methyl radical is an excellent electrophile in chemical reactions due to the incomplete octet. On the other hand, it can also act as a nucleophile with the single electron to participate in non-covalent interactions.

Both theoretical and experimental studies have proven that methyl radical with an unpaired electron plays a role of proton acceptor in the hydrogen-bonded complexes of $CH_3\cdots HF$,[6-9] $CH_3\cdots H_2O$,[6,10-13] $CH_3\cdots NH_3$,[6] $CH_3\cdots HCN$,[6,14-16] $CH_3\cdots HNC$,[14,16] and $CH_3\cdots HCCH$.[17] As expected, carbon radical is a poor hydrogen bond acceptor.[6] Wang et al.[17] named this new pattern of hydrogen bond as single-electron hydrogen bond, which is an interaction between the unpaired electron of a radical and the proton of hydrogen bond donor. Li et al.[11] predicted that there is a negative nonadditivity of methyl group in the single-electron hydrogen-bonded complex of $CH_3\cdots H_2O$. The single-electron hydrogen bond also exhibits cooperative effect with other types of hydrogen bonds in the complexes $CH_3\cdots HCN\cdots HCN$ and $CH_3\cdots HNC\cdots HNC$,[16] which has been addressed by binding distances, frequency shifts, interaction energies, NMR

chemical shifts, charge transfer, and electron densities. The hydrogen-bonded complexes involving radicals show different topological behaviors from the ones composed of neutral molecules,[6] even though both types of which exhibit the same spectroscopic properties. Besides, the methyl radical could serve as an electron donor to interact with lithium, sodium, halogen, and pnicogen atoms, consequently, leading to the formation of single-electron lithium,[18] sodium,[19] halogen,[20] and pnicogen bonds[21], respectively. The single-electron halogen bond shows a positive nonadditivity of methyl group,[22] which is different from the negative one in the hydrogen-bonded complex $CH_3\cdots H_2O$.[11] An ab initio study was performed to compare the single-electron hydrogen, lithium, and halogen bonds by applying HBe, H_2B, and H_3C radicals as the electron donors, and the results showed that the interactions become stronger in order of H_3C < HBe < H_2B.[23]

Single-electron halogen and pnicogen bonds belong to σ-hole interaction, which is an attractive interaction between the Lewis bases and σ-hole, a region of positive electrostatic potential on the outer side of the halogen and pnicogen atoms.[24-27] A similar σ-hole was also found on the surface of group IV atoms,[28] and the corresponding σ-hole interaction was considered to be the presence of one tetrel bond.[29] It was predicted that tetrel bonding interaction might play an important role in crystal materials and chemical reactions.[29-31] Recently, some theoretical studies have focused on the characteristics of the tetrel bonding interactions.[32,33] However, most of the Lewis bases in these tetrel-bonded complexes are related to neutral molecules and anions both with lone-pair electrons. On the basis of the similar characteristics of hydrogen bond

and σ-hole interactions, we are particularly interested in the interaction of the complexes composed of radicals and σ-hole. By analogy with single-electron hydrogen bond, it is reasonable to consider the existence of single-electron tetrel bond. Therefore, the prediction and characterization of the "single-electron tetrel bond" should be a meaningful work.

In the present paper, the complexes $FXH_3\cdots CH_3$ (X = C, Si, Ge, and Sn) were investigated by performing quantum chemical calculations to figure out the nature of the interaction between FXH_3 and methyl radical. Both atoms-in-molecules (AIM) electron topological and non-covalent interaction (NCI) index analyses were carried out to characterize single-electron tetrel bond. In order to gain a deeper understanding of the essential feature of this interaction, we further perform the energy decomposition analysis to estimate the strength of the interaction considering the attractive and repulsive contributions in a physically meaningful way in combination of natural bond orbital (NBO) calculation which refers to the delocalization interactions between the filled bonding orbitals of methyl radical and vacant antibonding ones of FXH_3. Finally, we will focus on the interplay of this interaction not only with hydrogen bond in $NCH\cdots NCCH_3\cdots CH_3$ complex, but also with conventional tetrel bond in $NCCH_3\cdots NCCH_3\cdots CH_3$.

2. Theoretical methods

All calculations were performed with Gaussian 09 program.[34] The structures of complexes $NCH\cdots NCCH_3$ and $NCCH_3\cdots NCCH_3$ were optimized at the MP2 level and those of complexes involved with radicals were optimized at the UMP2 level with

triple-zeta Dunning's augmented correlation consistent basis set aug-cc-pVTZ[35-37] for all atoms except Sn, for which the basis set aug-cc-pVTZ-PP[38] was used to take into account the relativistic effects. This method has been used to study single-electron hydrogen [14], lithium [18], halogen [22], and pnicogen [21] bonds. However, the MP2 method was used for closed-shell systems. The minimum energy structures of the complexes were confirmed by performing the harmonic vibrational frequency calculations. The interaction energy was estimated at the UCCSD(T)/aug-cc-pVTZ level by the supermolecular method as the difference between the energy of the complex and the sum of the energies of the isolated monomers in their equilibrium structures, which were optimized at the UMP2/aug-cc-pVTZ level. The counterpoise method of Boys and Bernardi[39] was applied to correct the basis set superposition error (BSSE) introduced by this strategy of evaluating interaction energy. Energy decomposition analysis (EDA) within the GAMESS program[40] was performed to get a deeper insight into the nature of this new pattern of the intermolecular interaction.

Molecular electrostatic potential (MEP) was calculated with the Wave Function Analysis-Surface Analysis Suite (WFA-SAS) program.[41] The natural bond orbital (NBO) method was used to analyze the delocalization interactions between the occupied and empty orbitals via the NBO program[42] implemented in Gaussian 09. For the complexes studied in this work, the topological parameters including the electron densities, Laplacians, and energy densities at the bond critical points (BCPs) were calculated using AIM2000 program.[43] The non-covalent interaction (NCI) index analysis was also done with the Multiwfn program,[44] and the related plots were graphed

with VMD program.[45]

3. Results and discussion

3.1. Existence of single-electron tetrel bond

The optimized structures of complexes $FXH_3\cdots CH_3$ (X = C, Si, Ge, and Sn) were depicted in Figure 1, which exhibit staggered conformation with C_{3v} symmetry. The C-H bond length of the methyl radical is 1.075 Å and 1.080 Å at the UMP2/aug-cc-pVTZ and UCCSD(T)/aug-cc-pVTZ levels, respectively, which are close to the experimental value 1.079 Å.[46] In these structures, the *p* orbital with single electron of carbon atom in the methyl radical points toward the X atom of FXH_3 with C–F bond in an opposite direction. The C···X distance is smaller (Table 1) than the sum of van der Waals Radii of the respective atoms,[47] indicative of an attractive interaction between both molecules. It is interesting that the C···X distance becomes shorter with the increase of the X atomic radius, which implies the stronger interactions of the complexes with larger atomic number of X. The unpaired electron of the methyl radical could shift the electron density toward the σ-hole on the X atom in FXH_3, as depicted in the electrostatic potential map of FCH_3 in Figure 2. That is, the single electron of methyl radical is attracted to the σ-hole of X. We name this interaction as "single-electron tetrel bond" in view of the concepts of tetrel bond[32,33] and single-electron hydrogen bond.[17] The existence of single-electron tetrel bond can be evidenced by the presence of C···X BCP in the complexes $FXH_3\cdots CH_3$ (X = C, Si, Ge, and Sn), as shown in Figure 3. It was demonstrated that NCI index is a powerful means for predicting weak non-covalent interactions.[48,49] This method has been used to study

hydrogen bonds[48,49] and halogen bonds.[50] Plot of the reduced density gradient (RDG) versus sign(λ_2)ρ for the complex exhibits the characteristic feature of one spike in the low-energy, low-density region (Figure 4), a typical footprint of non-covalent interactions. Thus, the NCI index can also predict the existence of the single-electron tetrel bond. Here, we analyzed the interactions of the single-electron tetrel bond in $FXH_3\cdots CH_3$ (X = C, Si, Ge, and Sn) with this index. Although the shape of the NCI region is similar for four complexes $FXH_3\cdots CH_3$ (X = C, Si, Ge, and Sn), the location of the spike has a greater deviation from the zero and the sharp of the spike becomes broader with the increase of the X atomic number, which is consistent with the variational trend of the interaction strength.

3.2. Characteristics of single-electron tetrel bond

It is predictable from the characteristics of the single-electron hydrogen bonds that the single-electron tetrel bond interaction in these complexes is weak with small interaction energy. To obtain more accurate and reliable interaction energies, a single point energy was calculated at the UCCSD(T)/aug-cc-pVTZ level which presented a more negative interaction energy of the complexes compared to that using the UMP2/aug-cc-pVTZ method except $NCCH_3\cdots CH_3$ (Table 1). This is similar with that in single-electron hydrogen bonds.[17] The difference of the interaction energy at both levels is less than 0.61 kJ/mol, which shows a maximum deviation of less than 10% from the UCCSD(T) results. This indicates that the UMP2 method is also feasible for description of single-electron tetrel bond.

The interaction energy of the complexes $FXH_3\cdots CH_3$ (X = C, Si, Ge, and Sn)

becomes more negative with the increase of the atomic number of X (Table 1), which shows a good linear relationship with the positive ESP value of σ-hole on the X atom in FXH_3 (Figure 2). This indicates that electrostatic interaction makes a positive contribution to the strength of single-electron tetrel bond interaction between FXH_3 and methyl radical. The interaction energy of -9.16 kJ/mol in the complex $FSnH_3\cdots CH_3$ is less negative than that in $FH\cdots CH_3$ at the UCCSD(T)/aug-cc-pVTZ level,[17] which demonstrates that the σ-hole on the X atom in FXH_3 is a weak electron acceptor.

As shown in Table 1, the F–X bond in complexes $FXH_3\cdots CH_3$ (X = C, Si, Ge, and Sn) is lengthened compared with that in the monomer FXH_3, which implies that the bond strength of F–X becomes weak arising from the formation of the single-electron tetrel bond. The delocalized interaction between the single-electron occupied *p* orbital in the methyl radical and the F–X antibonding orbital in FXH_3 provides strong support for the bond elongation of F–X. The similar orbital interaction was also found in the tetrel-bonded complex of $FCH_3\cdots CH_3OH$.[32] The energies of delocalized interaction were estimated to be in the range of 2.05 ~ 20.82 kJ/mol for complexes $FXH_3\cdots CH_3$ (X = C, Si, Ge, and Sn) with second-order perturbation energy as shown in Table 2, exhibiting a linear relationship with the variation of the interaction energy, that is, the delocalized orbital interaction is important for the stability of the tetrel-bonded complexes. The orbital interaction in the single-electron tetrel bond is comparable in strength to that in conventional ones.[32] To have a precise measure for the shift of charge density in the formation of the single-electron tetrel bond, the maps of electron density difference for all complexes were plotted in Figure 5. An increase of electron density

(red area) is observed for the single-electron occupied *p* orbital of the methyl radical, with a decrease (blue region) in the σ-hole on the X of XH_3 group. Both regions are getting larger and closer with the increase of the X atomic number, which are consistent with the fact that charge transfer in $FCH_3\cdots CH_3$ complex is the smallest while $FSnH_3\cdots CH_3$ has the largest one (Table 2). This feature is similar with that observed in hydrogen bonds.[52]

Accompanied with the bond elongation, the F–X (X = C, Si, Ge, and Sn) stretch vibration exhibits a small red shift, which is difficult to be observed with infrared spectroscopy. To figure out this problem, more stable radicals should be used to interact with FXH_3. It was known that (2,2,6,6-tetramethylpiperidin-1-yl)oxy (TEMPO) is a stable radical.[52] Here, the complex composed of TEMPO and FCH_3 was shown in Figure 6, with moderate interaction energy of -12.36 kJ/mol at the UMP2/aug-cc-pVDZ level. The C–F bond is lengthened by 0.008 Å with the corresponding stretch vibration exhibiting a red shift of 24 cm^{-1}.

Mani and Arunan[32] analyzed the topological parameters of a series of the complexes involving the tetrel bonds, confirming that a set of criteria for C–H···O hydrogen bonds on the basis of AIM theory proposed by Koch and Popelier is also feasible for tetrel bonds. The single-electron tetrel bond interaction was also analyzed with the AIM theory and the related results were presented in Table 3. The values of electron density and its Laplacian are positive in the ranges of 0.0028 ~ 0.0114 au and 0.0113 ~ 0.0296 au, respectively, both of which are in accord with the criteria suggested for hydrogen bonds.[53] It was shown that electron density can be used to measure the strength of

hydrogen bond.[54] This conclusion is also tenable for the single-electron tetrel bond interaction, which is confirmed by the fact that the electron density at the C···X BCP exhibits a linear relationship with the interaction energy. The energy density (H) is another important topological parameter due to fact that the type of interaction is related to its sign: a positive H corresponds to a purely closed shell interaction and a negative one to covalent interaction.[55] Thus, the positive H at the C···X BCP in these complexes means that the single-electron tetrel bond belongs to purely closed shell interactions.

3.3. Nature of single-electron tetrel bond

To obtain the physical pictures of the single-electron tetrel bond interaction, we applied the localized molecular orbital energy decomposition analysis (LMOEDA),[56] which provides the interaction energy as a sum of electrostatic (E^{ele}), exchange (E^{ex}), repulsion (E^{rep}), polarization (E^{pol}), and dispersion (E^{disp}) contributions. The results are listed in Table 4. The interaction energy of the complexes obtained by LMOEDA approach is approximately equal to that by the supermolecular method. This indicates that LMOEDA is reliable for analyzing the interaction energy of single-electron tetrel bond. The polarization term E^{pol} has the smallest contribution to the total interaction energy, indicating a weak perturbation of electron density distribution arising from the weak interaction in these single-electron tetrel-bonded complexes. In the complexes of $YCH_3\cdots CH_3$ (Y = CN, NC, NO_2), the magnitudes of E^{ele} are nearly equal to that of E^{disp}, while in the complexes $FXH_3\cdots CH_3$ (X = Si, Ge, Sn), the former has larger contribution to the total interaction energy than the latter. The larger E^{ele} corresponds to a bigger orbital overlapping between both molecules, and is also consistent with the conclusion

that there is a linear relationship between the electrostatic potential on the σ-hole of X atom and the interaction energy. With the increase of the X atomic number in $FXH_3\cdots CH_3$ (X = C, Si, Ge, and Sn), both E^{ele} and E^{disp} terms become more negative with the former even more remarkable. The relatively large E^{ex} and E^{rep} terms indicate that there is a significant orbital overlap between the two molecules in the complexes.

3.4. Substituent effect

The above results demonstrate that single-electron tetrel bond is a weak non-covalent interaction. According to the fact that electron-withdrawing groups in the proton donor can strengthen hydrogen bonds,[57] it is interesting to reveal the influence of the substituents on the interaction strength of single-electron tetrel bond. F atom in $FCH_3\cdots CH_3$ complex was replaced by strong electron-withdrawing groups -CN, -NC, and $-NO_2$, respectively. As can be seen from Table 1, the interaction energies in the complexes $NCCH_3\cdots CH_3$, $CNCH_3\cdots CH_3$, and $O_2NCH_3\cdots CH_3$ are more negative than that in $FCH_3\cdots CH_3$ complex at the UMP2/aug-cc-pVTZ level, which was confirmed by the ESP value of the σ-hole on the C atom in the molecules YCH_3 (Y = F, CN, NC, NO_2). This implies that the electron-withdrawing groups in the Lewis acid enhance the strength of single-electron tetrel bond similar with that in hydrogen bonds. However, the C···C distance becomes longer in the complexes $NCCH_3\cdots CH_3$, $CNCH_3\cdots CH_3$, and $O_2NCH_3\cdots CH_3$ compared with that in $FCH_3\cdots CH_3$ complex, which is inconsistent with the interaction energy, the perturbation energy of $LP_C\rightarrow BD^*_{Y\text{-}C}$ orbital interaction as well as the electron density at the C···X BCP.

On the other hand, the methyl group plays a significant role in hydrogen bonds[58]

and can exhibit nonadditivity effect in the hydrogen bond interactions.[11] It would be interesting to have a deeper view of this effect on the single-electron tetrel bond. Hence, the hydrogen atoms in the methyl radical are substituted stepwise by 1~3 methyl groups, respectively. The corresponding structures are shown in Figure 7 with the interaction energies listed in Table 5. The interaction energy of $FCH_3\cdots CH_2CH_3$ complex is -4.64 kJ/mol, which is more negative than that of $FCH_3\cdots CH_3$, indicating a positive role of methyl substituent of the methyl radical in enhancing the strength of the single-electron tetrel bond interaction. This is in agreement with the fact that the methyl group in the Lewis base is electron-donating in hydrogen bonds.[11] As is expected, with the increase of the number of methyl groups in methyl radical, the interaction energy becomes more negative. This evidences that the methyl substituents in methyl radical also exhibits nonadditivity effect in enhancing the strength of the single-electron tetrel bond, furthermore, it is negative nonadditivity, which is evidenced by the decreasing contribution of each following methyl substituent to the interaction strength. This is similar to that in the single-electron hydrogen bond.[11]

3.5. Competition

In addition to formation of the weak hydrogen-bonded complex, it has been confirmed that the methyl radical can form strong covalent-bonded complex with hydrogen cyanide and hydrogen iso-cyanide.[14] In our previous study, we have compared the acidity of the proton in methane and the methyl radical and found that the methyl radical is easier to provide proton.[59] As a consequence, we presented the optimized structures of complexes in Figure 8, where methyl radical plays the role of

proton donor combining with NC group in $NCCH_3$ and CN group in $CNCH_3$.

Both cases that NC group in $NCCH_3$ and CN group in $CNCH_3$ interact with carbon atom of the methyl radical gave rise to the same geometric structure. In this structure, C2···C3 distance is 1.490 Å, while the N···C1 distance is 1.451 Å, both of which are far shorter than the sum of cutoff distance of the both atoms for van der Waals interactions but close to the sum of their covalent radius (1.54 Å for two C atoms and 1.52 Å for C and N atoms). On the other hand, they are longer than the lengths of C–C and N–C single bonds in the monomers $NCCH_3$ and $CNCH_3$, which are 1.457 Å and 1.421 Å, respectively. Thus, the C2···C3 and N···C2 interactions are partially covalent character.[14] This strong interaction leads to a prominent deviation from the plane structure of the methyl radical in the complex. This structure was expected to be the global minimum of the potential surface of the complexes composed of the methyl radical and molecule $NCCH_3$ or $CNCH_3$.

It is noteworthy to see that the hydrogen-bonded complex between the methyl radical and $CNCH_3$ has the interaction energy of -4.06 kJ/mol with H···C distance of 2.752 Å. This interaction energy of hydrogen-bonded isomer is comparable to that of the corresponding single-electron tetrel-bonded one. The similar result was found in the hydrogen-bonded complex of $H_2CH\cdots NCCH_3$. Undoubtedly, there is a competition of the formation of both hydrogen-bonded and the single-electron tetrel-bonded complexes.

3.6. Synergistic effect

Synergistic effect is an important property of non-covalent interaction and has

attracted much attention because it plays a significant role in the supermolecular chemistry.[60] In the present study, we found that the synergistic effect involved with single-electron tetrel bonds is also nonnegligible. We introduced another molecule NCH or $NCCH_3$ into the structure of complex $NCCH_3\cdots CH_3$, giving rise to the structures of the trimers, as shown in Figure 9. In the trimer $NCH\cdots NCCH_3\cdots CH_3$, besides one single-electron tetrel bond, there is a C-H···N hydrogen bond. However, the single-electron tetrel bond coexists with a conventional tetrel bond in $NCCH_3\cdots NCCH_3\cdots CH_3$. In both trimers, the single-electron tetrel bond is marked as 2, with the other interaction represented by 1. The geometrical parameters and energy are collected in Table 6. The binding distances in the trimers are shorter, and the interaction energies are more negative with respect to those in the related dimers. This indicates that in the multi-component complex, the single-electron tetrel bond can interplay with the coexisted hydrogen bond or conventional tetrel bond. The binding distance of the single-electron tetrel bond has greater shortening than that of the hydrogen bond and conventional tetrel bond due to the weaker strengthen of single-electron tetrel bond compared to that of hydrogen bond and conventional tetrel bond. In the trimer $NCH\cdots NCCH_3\cdots CH_3$, the interaction energy of the single-electron tetrel bond is increased by 18.4%, while by only 2.2% for that of the hydrogen bond. A similar variation is found for the interaction energies in $NCCH_3\cdots NCCH_3\cdots CH_3$ trimer. The synergistic effect can be further evidenced by the negative cooperative energy, although its value is small. The cooperative energy corresponds to about 1.9% and 6.4% of the total interaction energy in $NCH\cdots NCCH_3\cdots CH_3$ and $NCCH_3\cdots NCCH_3\cdots CH_3$ trimers,

respectively. The synergistic effect involved with the single-electron tetrel bond is similar with that in hydrogen bonds.[16]

4. Conclusions

The monomers FXH_3 with X being the IV Group atoms have been evidenced to act as Lewis acids to interact with the single electron in the methyl radical. This new type of interaction is named as single-electron tetrel bond. It shares some similarities with hydrogen bonds, although some differences are also found between them. The single-electron tetrel bond is weak with small interaction energy, where the dispersion and electrostatic terms make approximately equal contributions in the weak tetrel bond interaction, while the latter plays a dominant role in the relatively strong one. The strong electron-withdrawing substituents in the monomer of electron acceptor can strengthen the single-electron tetrel bond. On the other hand, the methyl substituents in the Lewis base also exhibit an enhancing effect on the strength of single-electron tetrel bond interaction, and a negative nonadditivity is found among the substituent methyl groups. The single-electron tetrel bond can compete with the hydrogen bond in the complexes of $NCCH_3\cdots CH_3$ and $CNCH_3\cdots CH_3$. It also shows cooperative effect with other types of interactions. These results are important for the applications in molecular recognition and supermolecular chemistry involving single-electron tetrel bonds.

Acknowledgements

This work was supported by the Outstanding Youth Natural Science Foundation of Shandong Province (JQ201006), the Program for New Century Excellent Talents in University, the Key Project of Natural Science Foundation of Shandong Province of

China (ZR2013HZ004), and Open Project of State Key Laboratory of Supramolecular Structure and Materials (sklssm201418).

References

1. J. A. Kulkarni and K. D. Asgaonkar, *Int. J. Res. Pharm. Biomed. Sci.,* 2012, **3**, 325-351.
2. B. Bezard, P. N. Romani, H. Feuchtgruber and T. Encrenaz, *Astrophys. J*., 1999, **515**, 868-872.
3. D. M. Chipman, *J. Chem. Phys*., 1983, **78**, 3112-3132.
4. G. Buscarino S. Agnello, F.M. Gelardi and R. Boscaino, *J. Non-Cryst. Solids*, 2013, **361**, 9-12.
5. D. S. Marynick and D. A. Dixon, *Proc. Nati. Acad. Soc. USA*, 1977, **74**, 410-413.
6. I. Alkorta, I. Rozas and J. Elguero, *Ber. Bunsen. Phys. Chem*., 1998, **102**, 429-435.
7. H. Tachikawa, *J. Phys. Chem. A*, 1998, **102**, 7065-7069.
8. E. Y. Misochko, V. A. Benderskii, A. U. Goldschleger, A. V. Akimov and A. F. Shestakov, *J. Am. Chem. Soc.,* 1995, **117**, 11997-11998.
9. J.M. Merritt, S. Rudić and R.E. Miller, *J. Chem. Phys*., 2006, **124**, 084301.
10. S. Rudić, J.M. Merritt and R.E. Miller, *Phys. Chem. Chem. Phys.*, 2009, **11**, 5345-5352.
11. Q.Z. Li, H.J. Zhu, X.L. An, B.A. Gong and J.B. Cheng, *Int. J. Quantum Chem.*, 2009, **109**, 605-611.
12. S. Hammerum, *J. Am. Chem. Soc.*, 2009, **131**, 8627-8635.
13. X.L An, H.P. Liu, Q.Z. Li, B.A. Gong and J.B. Cheng, *J. Phys. Chem. A*, 2008, **112**, 5258-5263.
14. M. Solimannejad and M.E. Alikhani, *Chem. Phys. Lett.*, 2005, **406**, 351-354.
15. S. Rudić, J.M. Merritt and R.E. Miller, *J. Chem. Phys.*, 2006, **124**, 104305.
16. Q.Z. Li, X.L. An, F. Luan, W.Z. Li, B.A. Gong, J.B. Cheng and J.Z. Sun, *J. Chem. Phys.*, 2008, **128**, 154102.
17. B.Q. Wang, Z.R. Li, D. Wu, X.Y. Hao, R.J. Li and C.C. Sun, *Chem. Phys. Lett.*, 2003, **375**, 91-95.

18. Y. Li, D. Wu, Z.R. Li, W. Chen and C.C. Sun, *J. Chem. Phys.*, 2006, **125**, 084317.
19. Z.F. Li, Y.C. Zhu and H.X. Li, *Phys. Chem. Chem. Phys.*, 2009, **11**, 11113-11120.
20. Y.H. Wang, J.W. Zou, Y.X. Lu, Q.S. Yu and H.Y. Xu, *Int. J. Quantum Chem.*, 2007, **107**, 501-506.
21. I. Alkorta, J. Elguero and M. Solimannejad, *J. Phys. Chem. A*, 2014, **118**, 947-953.
22. Q.Z. Li, X.L. An, B.A. Gong and J.B. Cheng, *J. Mol. Struct: THEOCHEM*, 2008, **866**, 11-14.
23. Q.Z. Li, R. Li, S.C. Yi, W.Z. Li and J.B. Cheng, *Struct. Chem*., 2012, **23**, 411-416.
24. P. Politzer, J. S. Murray and T. Clark, *Phys. Chem. Chem. Phys.*, 2010, **12**, 7748–7757.
25. Q.Z. Li, R. Li, X.F. Liu, W.Z. Li and J.B. Cheng, *J. Phys. Chem. A*, 2012, **116**, 2547-2553.
26. T. Clark, M. Hennemann, J. S. Murray and P. Politzer, *J. Mol. Model.*, 2007, **13**, 291-296.
27. P. Politzer, P. Lane, M. C. Concha, Y.G. Ma and J. S. Murray, *J. Mol. Model*., 2007, **13**, 305-311.
28. J. S. Murray, P. Lane and P. Politzer, *J. Mol. Model.*, 2009, **15**, 723-729.
29. A. Bauza, T. J. Mooibroek and A. Frontera, *Angew. Chem. Int. Ed.*, 2013, **52**, 12317-12321.
30. S. J. Grabowski, *Phys. Chem. Chem. Phys*., 2014, **16**, 1824-1834.
31. N. W. Mitzel, A. J. Blake and D. W. H. Rankin, *J. Am. Chem. Soc*., 1997, **119**, 4143-4148.
32. D. Mani and E. Arunan, *Phys. Chem. Chem. Phys.*, 2013, **15**, 14377-14383.
33. D. Mani and E. Arunan, *ChemPhysChem*, 2013, **14**, 754-763.
34. M. J. Frisch, G. W. Trucks, H. B. Schlegel, G. E. Scuseria, M. A. Robb, J. R. Cheeseman, G. Scalmani, V. Barone, B. Mennucci, G. A. Petersson, H. Nakatsuji, M. Caricato, X. Li, H. P. Hratchian, A. F. Izmaylov, J. Bloino, G. Zheng, J. L. Sonnenberg, M. Hada, M. Ehara, K. Toyota, R. Fukuda, J. Hasegawa, M. Ishida, T. Nakajima, Y. Honda, O. Kitao, H. Nakai, T. Vreven, J. J. A. Montgomery, J. E. Peralta, F. Ogliaro, M. Bearpark, J. J. Heyd, E. Brothers, K. N. Kudin, V. N.

Staroverov, R. Kobayashi, J. Normand, K. Raghavachari, A. Rendell, J. C. Burant, S. S. Iyengar, J. Tomasi, M. Cossi, N. Rega, J. M. Millam, M. Klene, J. E. Knox, J. B. Cross, V. Bakken, C. Adamo, J. Jaramillo, R. Gomperts, R. E. Stratmann, O. A. Yazyev, J. Austin, R. Cammi, C. Pomelli, J. W. Ochterski, R. L. Martin, K. Morokuma, V. G. Zakrzewski, G. A. Voth, P. Salvador, J. J. Dannenberg, S. A. Dapprich, D. Daniels, O. Farkas, J. B. Foresman, J. V. Ortiz, J. Cioslowski and D. J. Fox, Gaussian 09, Revision A.02, Gaussian, Inc., Wallingford CT, 2009.

35. D. E. Woon and T. H. Dunning, Jr., *J. Chem. Phys.*, 1994, **100**, 2975-2988.
36. D. E. Woon and T. H. Dunning, Jr., *J. Chem. Phys*., 1993, **98**, 1358-1371.
37. R. A. Kendall, T. H. Dunning, Jr. and R. J. Harrison, *J. Chem. Phys*., 1992, **96**, 6796-6808.
38. D. Feller, *J. Comp. Chem.*, 1996, **17**, 1571-1586.
39. S. F. Boys and F. Bernardi, *Mol. Phys*., 1970, **19**, 553-558.
40. M. W. Schmidt, K. K. Baldridge, J. A. Boatz, S. T. Elbert, M. S. Gordon, J. H. Jensen, S. Koseki, N. Matsunaga, K. A. Nguyen, S. J. Su, T. L. Windus, M. Dupuis and J. A. Montgomery, *J. Comput. Chem.*, 1993, 14, 1347-1363.
41. F. A. Bulat, A. Toro-Labbé, T. Brinck, J. S. Murray and P. Politzer, *J. Mol. Model.*, 2010, **16**, 1679-1691.
42. A. E. Reed, L. A. Curtiss and F. Weinhold, *Chem. Rev.*, 1988, **88**, 899–926.
43. R. F. W. Bader, AIM2000 Program, McMaster University, Hamilton, Canada, 2000.
44. T. Lu and F. Chen, *J. Comput. Chem.*, 2012, **33**, 580-592.
45. W. Humphrey, A. Dalke and K. Schulten, *J. Mol. Graphics*, 1996, **14**, 33-38.
46. S. Hix, M.B. Kadiis, R.P. Mason and O. Augusto, *Chem. Res. Toxicol*., 2000, **13**, 1056-1064.
47. N. L. Allinger, X. Zhou and J. Bergsma, *J. Mol. Struct: Theochem*, 1994, **312**, 69-83.
48. J. Contreras-Garca, E. R. Johnson, S. Keinan, R. Chaudret, J. P. Piquemal, D. N. Beratan and W. T. Yang, *J. Chem. Theory Comput*., 2011, **7**, 625-632.
49. E. R. Johnson, S. Keinan, P. Mori-Sanchez, J. Contreras-Garcia, A. J. Cohen and

W. T. Yang, *J. Am. Chem. Soc*., 2010, **132**, 6498-6506.

50. B. Pinter, N. Nagels, W. A. Herrebout and F. De Proft, *Chem. Eur. J*., 2013, **19**, 519-530.
51. S. Scheiner and T. Kar, *J. Phys. Chem. A*, 2002, **106**, 1784-1789.
52. F. Montanari, S. Quici, H. Henry-Riyad and T. T. Tidwell, Encyclopedia of Reagents for Organic Synthesis; John Wiley & Sons, 2005.
53. U. Koch and P. L. A. Popelier, *J. Phys. Chem. A*, 1995, **99**, 9747-9754.
54. P. Lipkowski, S. J. Grabowski, T.L. Robinson and J. Leszczynski, *J. Phys. Chem. A*, 2004, **108**, 10865-10872.
55. W. D. Arnold and E. Oldfield, *J. Am. Chem. Soc*., 2000, **122**, 12835-12841.
56. P. F. Su and H. Li, *J. Chem. Phys.*, 2009, **131**, 014102.
57. A. H. D. Lopez, G. F. Caramori, D. F. Coimbra, R. L. T. Parreira and É. H. da Silva, *ChemPhysChem*, 2013, **14**, 3994-4001.
58. Q.Z. Li, Z.W. Yu and G.S. Wu, *J. Am. Chem. Soc*., 2016, **128**, 1438-1439.
59. Q.Z. Li, H. Kou, R. Li, W.Z. Li and J.B. Cheng, *Comput. Theor. Chem*., 2011, 976, 83–87.
60. N. Lanigan and X. S. Wang, *Chem. Commun*., 2013, **49**, 8133-8144.

Table 1. Binding distance (R, Å), change of X–Y bond (Δr, Å) in complexes compared with that in monomers, shift of X–Y stretch frequency (Δv, cm^{-1}), and interaction energy (ΔE, kJ/mol) in the complexes of $YXH_3\cdots CH_3$ (X = C, Si, Ge, Sn; Y = F, CN, NC, NO_2) at the UMP2/aug-cc-pVTZ level.

	$R_{X\cdots C}$[a]	Δr_{X-Y}	Δv_{X-Y}	ΔE[b]
$FCH_3\cdots CH_3$	3.486[4.08]	0.000	-3	-2.80(-3.04)
$FSiH_3\cdots CH_3$	3.276[4.33]	0.004	-9	-5.91(-6.52)
$FGeH_3\cdots CH_3$	3.213[4.48]	0.006	-12	-6.47(-6.93)
$FSnH_3\cdots CH_3$	3.126[4.63]	0.009	-20	-8.73(-9.16)
$NCCH_3\cdots CH_3$	3.622	0.000	-2	-2.88(-2.64)
$CNCH_3\cdots CH_3$	3.517	0.001	-4	-3.42(-3.43)
$O_2NCH_3\cdots CH_3$	3.503	0.000	-1	-3.49(-3.73)

[a] The data in brackets are the sum of van der Waals Radii of the corresponding atoms [48].

[b] The data in parentheses are the interaction energies at the UCCSD(T)/aug-cc-pVTZ level based on the UMP2/aug-cc-pVTZ optimized geometries.

Table 2. Second-order perturbation energy (E^2, kJ/mol) and charge transfer (*CT*, me) in the complexes.

	E^2	*CT*
$FCH_3\cdots CH_3$	2.05	0.57
$FSiH_3\cdots CH_3$	9.20	9.97
$FGeH_3\cdots CH_3$	12.96	11.44
$FSnH_3\cdots CH_3$	20.82	22.07
$NCCH_3\cdots CH_3$	1.42	0.94
$CNCH_3\cdots CH_3$	2.17	1.24
$O_2NCH_3\cdots CH_3$	2.09	1.37

Table 3. Electron density (ρ), Laplacian ($\nabla^2\rho$), and energy density (*H*) at the intermolecular BCP in the complexes. All are in au.

	ρ	$\nabla^2\rho$	*H*
$FCH_3\cdots CH_3$	0.0033	0.0143	0.0009
$FSiH_3\cdots CH_3$	0.0067	0.0204	0.0006
$FGeH_3\cdots CH_3$	0.0080	0.0233	0.0006
$FSnH_3\cdots CH_3$	0.0114	0.0296	0.0003
$NCCH_3\cdots CH_3$	0.0028	0.0113	0.0007
$CNCH_3\cdots CH_3$	0.0032	0.0139	0.0009
$O_2NCH_3\cdots CH_3$	0.0033	0.0136	0.0009

Table 4. Energy decomposition for the complexes at the optimized equilibrium structures. All are in kJ/mol.

	E^{ele}	E^{ex}	E^{rep}	E^{pol}	E^{disp}	ΔE
$FCH_3\cdots CH_3$	-3.47	-7.98	13.13	-0.67	-3.72	-2.76
$FSiH_3\cdots CH_3$	-11.41	-27.21	45.39	-4.22	-8.69	-6.14
$FGeH_3\cdots CH_3$	-15.42	-33.06	56.81	-5.43	-9.24	-6.40
$FSnH_3\cdots CH_3$	-23.66	-50.24	87.65	-11.08	-10.91	-8.24
$NCCH_3\cdots CH_3$	-3.18	-6.14	10.12	-0.50	-3.14	-2.88
$CNCH_3\cdots CH_3$	-3.68	-7.73	12.79	-0.63	-4.14	-3.43
$O_2NCH_3\cdots CH_3$	-4.26	-7.19	12.04	-0.88	-3.26	-3.55

Table 5. Interaction energies (ΔE, kJ/mol) in the methyl-substituted complexes.

	ΔE	$\Delta\Delta E$	$\Delta\Delta E$/n
$FCH_3\cdots CH_3$	-2.80		
$FCH_3\cdots CH_2CH_3$	-4.64	-1.84	-1.84
$FCH_3\cdots CH(CH_3)_2$	-6.13	-3.33	-1.67
$FCH_3\cdots C(CH_3)_3$	-7.35	-4.55	-1.52

Note: $\Delta\Delta E$ is the difference of the interaction energy between in the methyl-substituted complex and in $FCH_3\cdots CH_3$ and n is the number of methyl group.

Table 6. Binding distances (R, Å), interaction energies (ΔE, kJ/mol), and cooperative energy (E_{coop}, kJ/mol) in the trimers.

	NCH···NCCH$_3$···CH$_3$	NCCH$_3$···NCCH$_3$···CH$_3$
R_1	2.126(2.127)[a]	3.176(3.187)[a]
R_2	3.596(3.622)[a]	3.608(3.622)[a]
ΔE_{total}	-27.72	-15.48
ΔE_1	-24.85(-24.32)[a]	-12.60(-12.29)[a]
γ_1[b]	2.2%	2.5%
ΔE_2	-3.41(-2.88)[a]	-3.21(-2.88)[a]
γ_2[b]	18.4%	11.4%
E_{coop}[d]	-0.52(1.9%)[c]	-0.31(6.4%)[c]

[a] The data in parentheses are from the corresponding dimers.

[b] γ is the increased percentage of the interaction energy in the trimer compared to that in the corresponding dimer.

[c] The data in parentheses are percentage of the E_{coop} to ΔE_{total}.

[d] E_{coop} is calculated with the formulas of $E_{coop} = \Delta E_{total} - \Delta E_1(D) - \Delta E_2(D)$, where ΔE_{total} is the total interaction energy in the trimer and $\Delta E(D)$ is the interaction energy in the dimer.

Figure captions

Figure 1. Optimized structures of $FXH_3\cdots CH_3$ (X = C, Si, Ge, and Sn) complexes. The right figure is plotted when the left one is observed from the right side.

Figure 2. Molecular electrostatic potentials of FCH_3. Color ranges, in eV, are: red, greater than 0.03; yellow, between 0.03 and 0; green, between 0 and -0.01; blue, less than -0.01.

Figure 3. Molecular graphs of complexes with the BCPs (red points).

Figure 4. Non-covalent interaction (NCI) regions (green disks) in $FXH_3\cdots CH_3$ (X = C, Si, Ge, and Sn) complexes.

Figure 5. Electron density shifts in $FXH_3\cdots CH_3$ (X = C, Si, Ge, and Sn) complexes. Red regions indicate increased density, blue regions indicate decreased density. Contours are shown at the 0.0002 au level.

Figure 6. Optimized structure of the complex of TEMPO and FCH_3 at the UMP2/aug-cc-pVDZ level.

Figure 7. Optimized structures of $FCH_3\cdots CH_2CH_3$, $FCH_3\cdots CH(CH_3)_2$, and $FCH_3\cdots C(CH_3)_3$ complexes.

Figure 8. Optimized structures of H_3CNCCH_3, $H_2CH\cdots CNCH_3$, and $H_2CH\cdots NCCH_3$ complexes.

Figure 9. Optimized structures of $NCH\cdots NCCH_3\cdots CH_3$ and $NCCH_3\cdots NCCH_3\cdots CH_3$ trimers

Figure 1

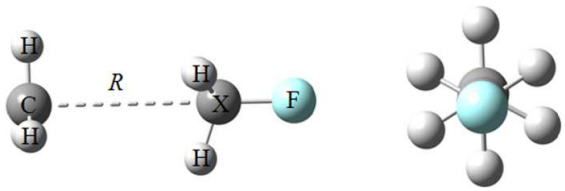

Figure 2

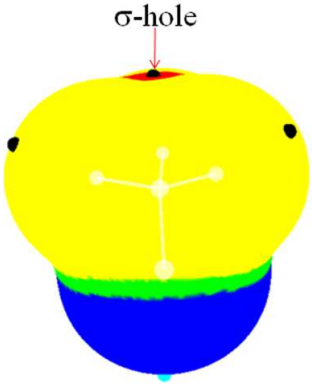

	V_{min}(eV)
FCH_3	0.0335
$FSiH_3$	0.0620
$FGeH_3$	0.0678
$FSnH_3$	0.0814
$NCCH_3$	0.0365
$CNCH_3$	0.0446
O_2NCH_3	0.0482

Figure 3

	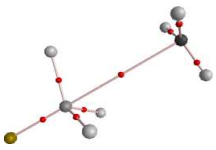
$FCH_3\cdots CH_3$	$FSiH_3\cdots CH_3$
	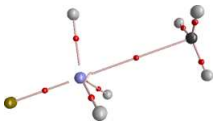
$FGeH_3\cdots CH_3$	$FSnH_3\cdots CH_3$
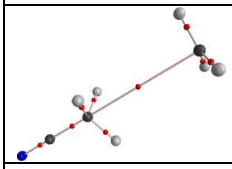	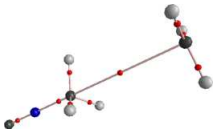
$NCCH_3\cdots CH_3$	$CNCH_3\cdots CH_3$
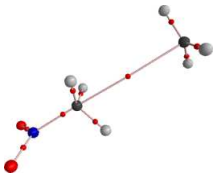	
$O_2NCH_3\cdots CH_3$	

Figure 4

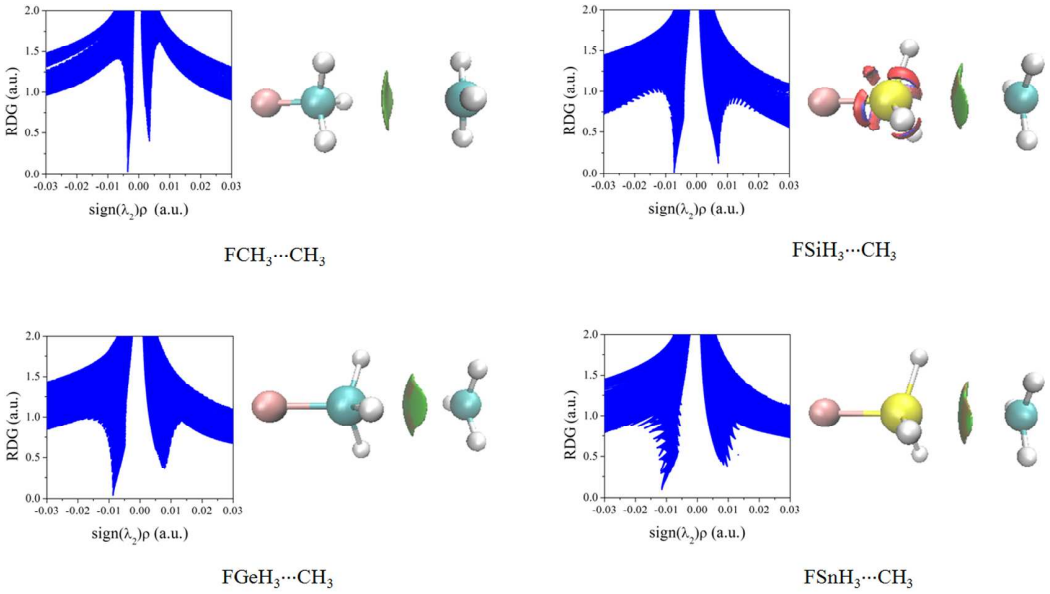

Figure 5

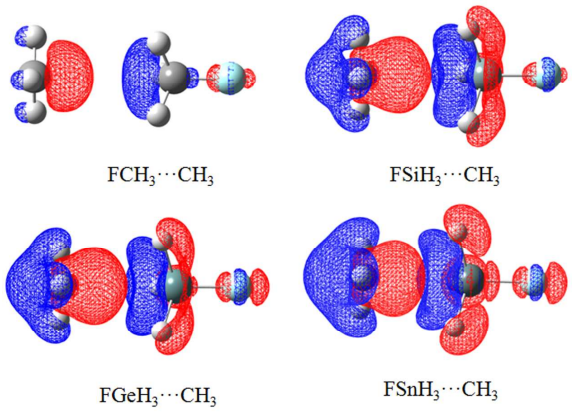

Figure 6

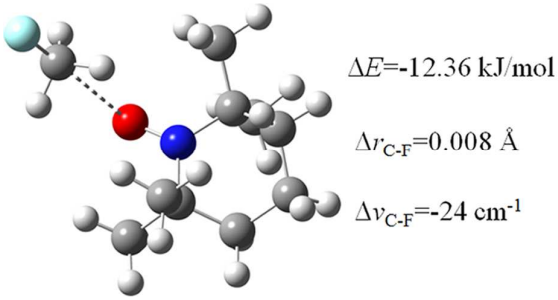

Figure 7

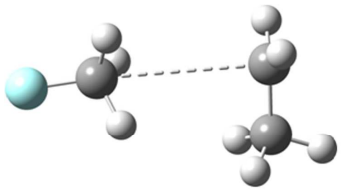

$FCH_3\cdots CH_2CH_3$

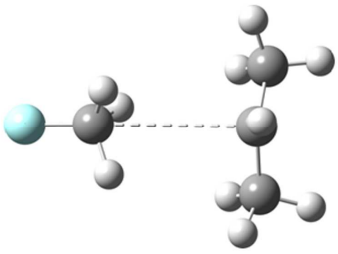

$FCH_3\cdots CH(CH_3)_2$

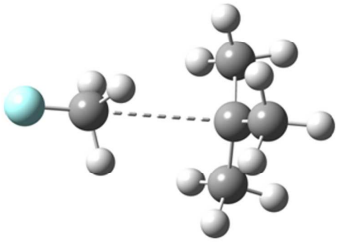

$FCH_3\cdots C(CH_3)_3$

Figure 8

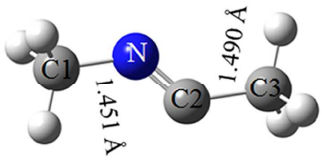

H_3CNCCH_3

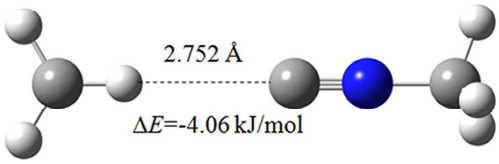

$H_2CH\cdots CNCH_3$

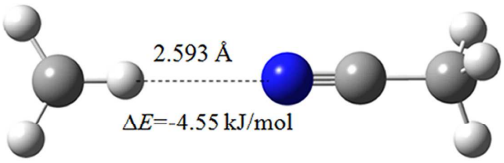

$H_2CH\cdots NCCH_3$

Figure 9

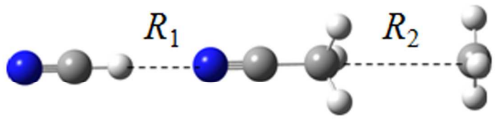

$NCH\cdots NCCH_3\cdots CH_3$

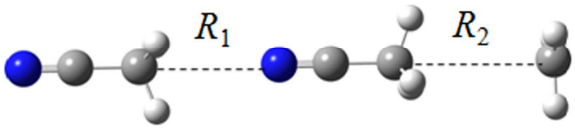

$NCCH_3\cdots NCCH_3\cdots CH_3$

TOC

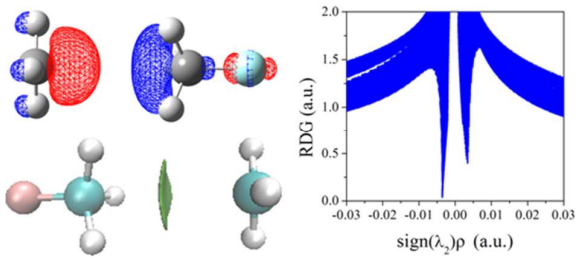

A single-electron tetrel bond was predicted and characterized in the complexes $FXH_3\cdots CH_3$ (X = C, Si, Ge, and Sn).